Synthesis and Analysis of a Reduced Size Planar Hybrid Ring

Marija Agatonović, Bratislav Milovanović

Abstract — **This paper presents a method for synthesis and analysis of a reduced size planar hybrid ring. Dimensions of the ring are reduced due to the slow-wave effect of capacitively loaded transmission line. Analysis formulas are derived using the symmetry of the reduced size model. Hybrid ring S-parameters are simulated and compared to the S-parameters of the conventional hybrid ring coupler. Phase differences between output ports are analysed for several lengths of transmission lines.**

Keywords — **Slow-wave effect, synthesis and analysis of the hybrid ring.**

I. INTRODUCTION

Hybrid ring coupler is a very important component in many communication systems. It is used in balanced mixers, frequency discriminators, amplifiers, power combainers, power splitters, modulators and antenna array feed networks. Hybrid ring is a four-port microwave network which has a function of in-phase and out-of phase power splitting. The power excited at one port is equally splitted and delivered to the neighbouring ports and no power appears at the fourth port. The conventional hybrid ring is composed of three quarter-wavelength transmission lines and one line with a length of $3\lambda/4$, at a center frequency (Fig. 1). Generally, characteristic impedances of the ports and ring are 50 Ω and 70.7 Ω, respectively. Small-size hybrid rings are frequently required in many applications. At the lower frequencies of the microwave band, the size of the conventional hybrid ring is too large for practical use. Also, it is unacceptable large for use in monolithic microwave integrated circuit (MMIC) as larger dimensions result in higher chip cost. Several technical solutions have been proposed to reduce the hybrid ring size. If every transmission line of the ring is replaced by an equivalent model with capacitors and inductors, a significant size reduction can be achieved, [1]. The complete lumped-element approach requires precise inductor values which increase fabriation difficulties.

Slow-wave effect of capacitively loaded transmission line is utilized to design a reduced size branch-line hybrid with arbitrary power splitting, [2]. In this paper, the reduced size hybrid ring coupler is presented. It consists of four

Marija Agatonović, Faculty of Electronic Engineering in Niš, Aleksandra Medvedeva 14, 18000 Niš, Serbia; (e-mail: magatonovic@gmail.com).

Bratislav Milovanović, Faculty of Electronic Engineering in Niš, Aleksandra Medvedeva 14, 18000 Niš, Serbia; (e-mail: batam@pogled.net).

capacitively loaded transmission lines. When lengths of the lines are reduced, their characteristic impedances are increased. Miniaturization level depends on the fabrication limits for high impedance transmission lines. If the thinner substrate is used, the greater reduction will be achieved. By decreasing transmission lines, the total size of microwave integated circuit can be reduced.

In the following text, scattering parameters and phase differences between output ports of the reduced size hybrid ring will be descibed and analysed.
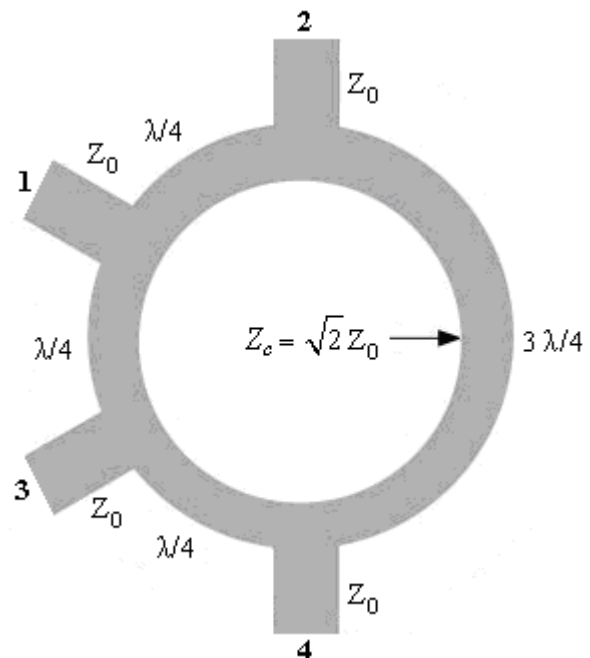
Fig. 1. Conventional hybrid ring

II. REDUCED SIZE HYBRID RING

Conventional hybrid ring consists of three quarter-wavelength transmission lines and one transmission line with length of $3\lambda/4$, [3]. Therefore, the circumference of the ring is $3/2\ \lambda$.
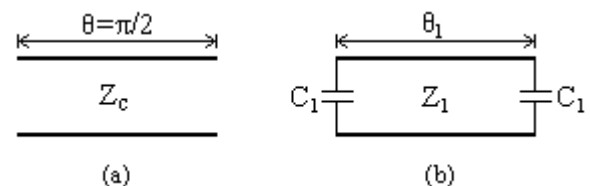
Fig. 2. Quarter-wavelength transmission line (a), capacitively loaded transmission line (b)

In order to reduce dimensions of the hybrid ring, transmission lines are replaced by capacitively loaded transmission lines with equivalent electrical parameters (Fig. 2). Electrical length of the quarter-wavelength transmission line is $\theta = \pi / 2$. Characteristic impedance of the line is Z_c. Fig. 3 shows the geometry of a reduced size hybrid ring.
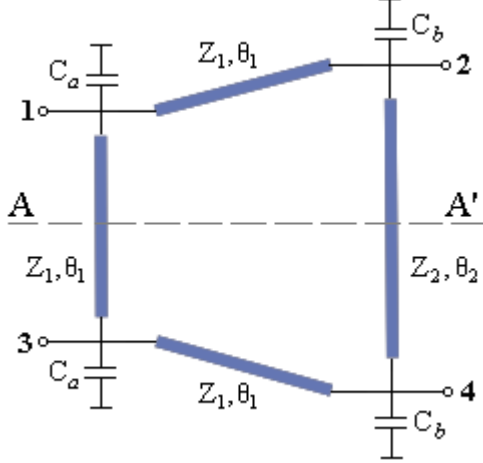
Fig. 3. Reduced size hybrid ring

The relations between the quarter-wavelength line and the reduced line can be estimated using ABCD matrices.

$$[ABCD] = \begin{bmatrix} \cos\theta & jZ_c \sin\theta \\ j\frac{1}{Z_c}\sin\theta & \cos\theta \end{bmatrix} = \begin{bmatrix} 0 & jZ_c \\ j\frac{1}{Z_c} & 0 \end{bmatrix} \quad (1)$$

$$[ABCD] = \begin{bmatrix} 1 & 0 \\ j\omega C_1 & 1 \end{bmatrix} \begin{bmatrix} \cos\theta_1 & jZ_1 \sin\theta_1 \\ j\frac{1}{Z_1}\sin\theta_1 & \cos\theta_1 \end{bmatrix} \begin{bmatrix} 1 & 0 \\ j\omega C_1 & 1 \end{bmatrix} \quad (2)$$

By equating ABCD matrices of the quarter-wavelength transmission line and capacitively loaded transmission line, equations for calculating values of Z_1 and C_1 are derived.

$$\cos\theta_1 - \omega C_1 Z_1 \sin\theta_1 = 0 \quad (3)$$

$$Z_1 \sin\theta_1 = Z_c \quad (4)$$

Similarly, equations for calculating characteristic impedance Z_2 and capacitance C_2 can be obtained.

$$[ABCD] = \begin{bmatrix} \cos\theta & jZ_c \sin\theta \\ j\frac{1}{Z_c}\sin\theta & \cos\theta \end{bmatrix} = \begin{bmatrix} 0 & -jZ_c \\ -j\frac{1}{Z_c} & 0 \end{bmatrix} \quad (5)$$

$$[ABCD] = \begin{bmatrix} 1 & 0 \\ j\omega C_2 & 1 \end{bmatrix} \begin{bmatrix} \cos\theta_2 & jZ_2 \sin\theta_2 \\ j\frac{1}{Z_2}\sin\theta_2 & \cos\theta_2 \end{bmatrix} \begin{bmatrix} 1 & 0 \\ j\omega C_2 & 1 \end{bmatrix} \quad (6)$$

$$\cos\theta_2 - \omega C_2 Z_2 \sin\theta_2 = 0 \quad (7)$$

$$Z_2 \sin\theta_2 = -Z_c \quad (8)$$

On the basis of Equations (4) and (8), we can see that impedances of capacitively loaded transmission lines are greater than those of the conventional hybrid ring coupler. Capacitances C_a and C_b can be determined using the following expressions

$$C_a = \frac{2}{\omega Z_c} \cos\theta_1 \quad (9)$$

$$C_b = \frac{1}{\omega Z_c} (\cos\theta_1 - \cos\theta_2). \quad (10)$$

Analysis of the reduced size hybrid ring can be performed using the symmetry of the component with respect to a line A-A', as depicted in Fig. 3. With appropriate excitations at hybrid ring ports, equations for S-parameters calculation can be derived. If two signals of amplitude 1/2 and in phase are applied at ports 1 and 3 (even-mode excitation), the magnetic wall is formed at A-A', [4]. This is equivalent to an open circuit, as indicated in Fig. 4.
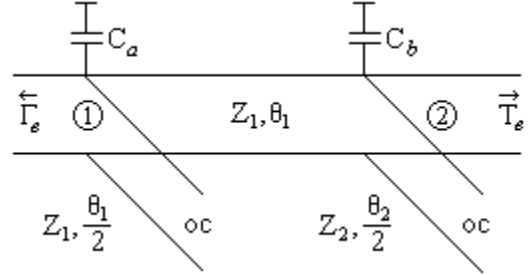
Fig. 4. Even-mode excitation

$$Y_a = j\omega C_a + j\frac{1}{Z_1}\tan\frac{\theta_1}{2} \text{ and } Y_b = j\omega C_b + j\frac{1}{Z_2}\tan\frac{\theta_2}{2}$$

$$\begin{bmatrix} A & B \\ C & D \end{bmatrix}_e = \begin{bmatrix} 1 & 0 \\ Y_a & 1 \end{bmatrix} \begin{bmatrix} \cos\theta_1 & jZ_1 \sin\theta_1 \\ j\frac{1}{Z_1}\sin\theta_1 & \cos\theta_1 \end{bmatrix} \begin{bmatrix} 1 & 0 \\ Y_b & 1 \end{bmatrix} \quad (11)$$

In a similar way, if two signals of amplitude 1/2 and 180° out of phase (odd-mode excitation) are applied at ports 1and 3, the electrical wall is created at A-A' (Fig. 5).
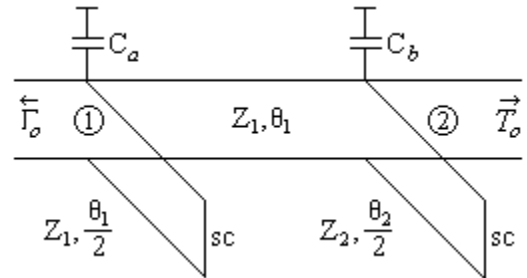
Fig. 5. Odd-mode excitation

$$Y_a = j\omega C_a - j\frac{1}{Z_1}\cot\frac{\theta_1}{2} \text{ and } Y_b = j\omega C_b - j\frac{1}{Z_2}\cot\frac{\theta_2}{2}$$

$$\begin{bmatrix} A & B \\ C & D \end{bmatrix}_o = \begin{bmatrix} 1 & 0 \\ Y_a & 1 \end{bmatrix} \begin{bmatrix} \cos\theta_1 & jZ_1 \sin\theta_1 \\ j\frac{1}{Z_1}\sin\theta_1 & \cos\theta_1 \end{bmatrix} \begin{bmatrix} 1 & 0 \\ Y_b & 1 \end{bmatrix} \quad (12)$$

The reflection and transmission coefficients for the even- and odd-mode are given by

$$\Gamma_{e,o} = \frac{A_{e,o} + B_{e,o} - C_{e,o} - D_{e,o}}{A_{e,o} + B_{e,o} + C_{e,o} + D_{e,o}} \quad (13)$$

$$T_{e,o} = \frac{2}{A_{e,o} + B_{e,o} + C_{e,o} + D_{e,o}} . \quad (14)$$

First row and column elements of the scattering matrix are determined on the basis of the following expressions

$$S_{11} = \frac{1}{2}\Gamma_e + \frac{1}{2}\Gamma_o, \ S_{21} = \frac{1}{2}T_e + \frac{1}{2}T_o, \ S_{31} = \frac{1}{2}\Gamma_e - \frac{1}{2}\Gamma_o \text{ and}$$

$$S_{41} = \frac{1}{2}T_e - \frac{1}{2}T_o .$$

When the even-mode excitation is applied at ports 4 and 2, there is the magnetic wall at A-A' (Fig. 6). Using [4], ABCD matrix for port 2 can be derived.
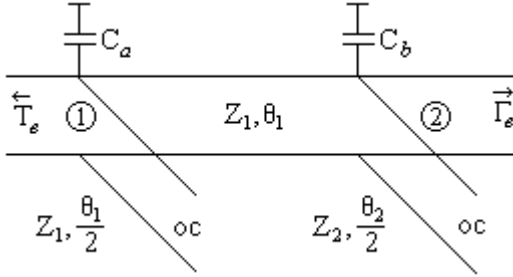
Fig. 6. Even-mode excitation

$$Y_a = j\omega C_a + j\frac{1}{Z_1}\tan\frac{\theta_1}{2} \text{ and } Y_b = j\omega C_b + j\frac{1}{Z_2}\tan\frac{\theta_2}{2}$$

$$\begin{bmatrix} A & B \\ C & D \end{bmatrix}_e = \begin{bmatrix} 1 & 0 \\ Y_b & 1 \end{bmatrix} \begin{bmatrix} \cos\theta_1 & jZ_1\sin\theta_1 \\ j\frac{1}{Z_1}\sin\theta_1 & \cos\theta_1 \end{bmatrix} \begin{bmatrix} 1 & 0 \\ Y_a & 1 \end{bmatrix} \quad (15)$$

The odd-mode excitation applied at ports 4 and 2, induces the electric wall to be formed at A-A'. Equivalent short circuit scheme is presented in Fig. 7. ABCD matrix for the odd mode can be found.
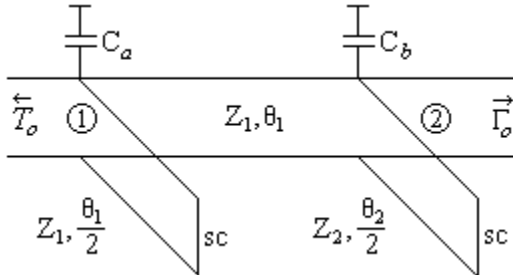
Fig. 7. Odd-mode excitation

$$Y_a = j\omega C_a - j\frac{1}{Z_1}\cot\frac{\theta_1}{2} \text{ and } Y_b = j\omega C_b - j\frac{1}{Z_2}\cot\frac{\theta_2}{2}$$

$$\begin{bmatrix} A & B \\ C & D \end{bmatrix}_o = \begin{bmatrix} 1 & 0 \\ Y_b & 1 \end{bmatrix} \begin{bmatrix} \cos\theta_1 & jZ_1\sin\theta_1 \\ j\frac{1}{Z_1}\sin\theta_1 & \cos\theta_1 \end{bmatrix} \begin{bmatrix} 1 & 0 \\ Y_a & 1 \end{bmatrix} \quad (16)$$

On the basis of ABCD matrices for the even- and odd-mode excitations, using (13) and (14), the reflection and transmission coefficients can be determined. Elements of the scattering matrix fourth row and column are determined using the following expressions $S_{14} = \frac{1}{2}T_e - \frac{1}{2}T_o$,

$$S_{24} = \frac{1}{2}\Gamma_e - \frac{1}{2}\Gamma_o, \ S_{34} = \frac{1}{2}T_e + \frac{1}{2}T_o \text{ and } S_{44} = \frac{1}{2}\Gamma_e + \frac{1}{2}\Gamma_o .$$

The rest od the elements in the scattering matrix can be found using the symmetry of the hybrid ring.

$$S_{ij} = S_{ji}, \quad i = 1,...,4, \quad j = 1,...,4 \quad (17)$$

Values of Z_1, Z_2, C_a, C_b, defined in (4), (8), (9) and (10), are calculated for chosen electrical lengths of the transmission lines. The resulting signals out of the four ports are a superposition of those obtained from the even- and odd- mode excitations. Finally, the calculated scattering matrix of the reduced size hybrid ring is equivalent to the one of the conventional hybrid coupler.

$$[S] = -\frac{j}{\sqrt{2}} \begin{bmatrix} 0 & 1 & 1 & 0 \\ 1 & 0 & 0 & -1 \\ 1 & 0 & 0 & 1 \\ 0 & -1 & 1 & 0 \end{bmatrix} \quad (18)$$

III. NUMERICAL RESULTS

Based on the derived equations in previous section the reduced size hybrid ring coupler can be simulated and analyzed. For different lengths of the transmission lines, scaterring parameters and phase differences between output ports are observed. On the basis of data from Table 1, simulations are completed using ADS (Agilent's Advanced Design System), with the following substrate parameters h=0.635mm, ε_r =2.32 and t=17μm.

TABLE 1. TRANSMISSION LINES IMPEDANCES AND CAPACITORS VALUES

l_1	l_2	Z_1, Ω	Z_2, Ω	$C_a(pF)$	$C_b(pF)$
λ/4	3λ/4	70.71	70.71	0	0
λ/5	4λ/6	74.35	81.65	1.39	1.82
λ/6	9 λ/14	81.65	90.44	2.25	2.53
λ/7	5 λ/8	90.44	99.99	2.81	2.99
λ/8	11 λ/18	99.99	110.01	3.18	3.32
λ/9	6 λ/10	110.01	120.29	3.45	3.55
λ/10	13λ/22	120.29	130.79	3.64	3.72
λ/11	7 λ/12	130.79	141.42	3.79	3.85
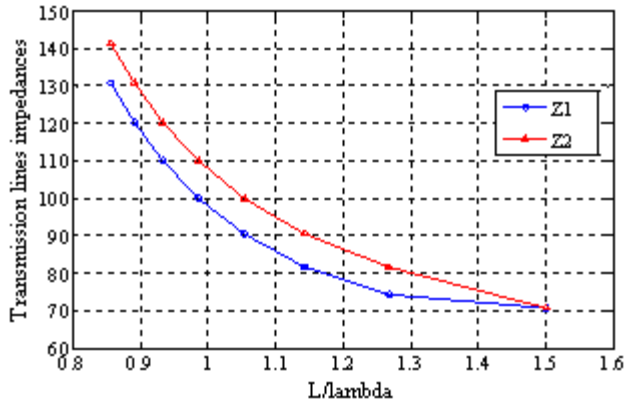
Fig. 8. Transmission line impedances versus the circumference of the ring
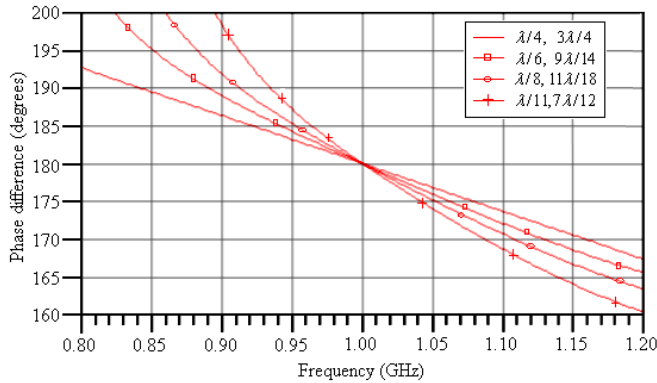
Fig. 9. Phase difference 180° at the output ports of the reduced size hybrid ring
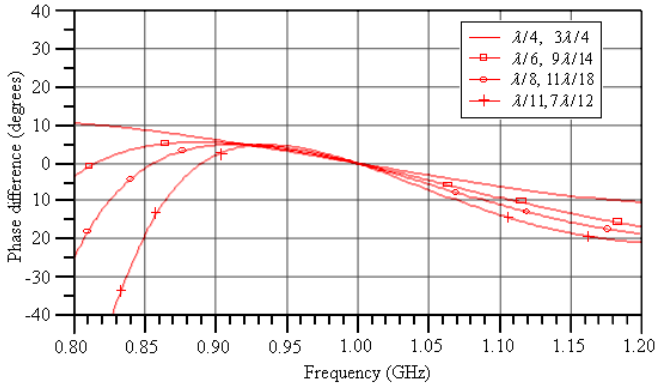
Fig. 10. Phase difference 0° at the output ports of the reduced size ring

As shown in Fig. 8, transmission line impedances depend on the circumference of the ring. When the value of L/λ decreases from 1.5 to 0.85, the circumference of the ring reduces by 43.33 %. If we continue reducing the lengths of transmission lines, their characteristic impedances get very high values that are difficult to realize in microwave integrated circuits. For the quarter-wavelength transmission line of 70.7 Ω at 1 GHz center frequency in hybrid ring, conventional microstrip should have a physical length of 54.484 mm. After embedding the capacitively loaded structure (λ/11), the length of the line can be decreased to 20.508 mm.

Because of the slow-wave effects of capacitively loaded

TABLE 2. FRACTIONAL BANDWIDTHS OF THE CONVENTIONAL AND REDUCED SIZE HYBRID RINGS

l_1	l_2	Isolation > 20dB	180°± 10°
λ/4	3λ/4	31.8 %	31.6 %
λ/5	4λ/6	31.6 %	26.5 %
λ/6	9 λ/14	25.4 %	24.0 %
λ/7	5 λ/8	20.6 %	21.5 %
λ/8	11 λ/18	17.6 %	19.6 %
λ/9	6 λ/10	15.3 %	18.0 %
λ/10	13λ/22	13.7 %	16.5 %
λ/11	7 λ/12	12.5 %	15.3 %

transmission lines, phase differences graphs are asymmetric in relation to the center frequency, (see Figs. 9 and 10). It can be clearly observed that decrease of transmission lines leads to slight increase of the graphs' slopes. It is shown in Fig. 9 that the smallest slope graph corresponds to the conventional hybrid ring. Phase differences can take values equal to zero at some frequencies that are lower than the operational one (Fig. 10).

For the reduced size hybrid ring, fractional bandwidth where phase difference fluctuate by ±10° is narrower than 31.8%. For instance, the reduced size model which consists of three sections of length λ/11 and one of length 7λ/12 has fractional bandwidth of 15,3%. At the center frequency, simulated S-parameter amplitudes $|S_{11}|, |S_{21}|, |S_{31}|$ and $|S_{41}|$, are -67.207 dB, -3.019 dB, -3.011 dB and -63.134 dB, respectively. The simulated return loss is better than 20 dB from 0.934 to 1.063 GHz. The simulated isolation is better than 20 dB from 0.954 to 1.074 GHz.

With a small frequency shift from the design center frequency, scattering parameters degrade rapidly and get values which are not acceptable for properly functioning of the hybrid ring. Further decrease of transmission lines lengths has a significant influence on phase differences at the output ports, which deviate and do not meet the requested values.

IV. CONCLUSION

The design of a planar reduced size hybrid ring has been described. The hybrid ring operating at 1 GHz consists of four capacitively loaded transmission lines. The design formulas have been obtained under ideal lossless situation. The circuits area of these coupler is smaller with good performances. Hybrid ring can be easily fabricated, making this design suitable for microwave integrated circuit (MIC) and MMIC applications.

REFERENCES

[1] M. Caulton, B. Hershenov, S.P. Knight and R.E. DeBrecht, "Status of lumped elements in microwave integrated circuits-present and future," IEEE Trans Microwave Theory Tech MTT-19 (1997), pp. 588-599
[2] M.V. Nedelchev, I.G. Iliev, "Synthesis and Analysis of Reduced-Size Branch-Line Hybrids," Microwave Review vol. 14, pp. 16-19
[3] Collin, Foundations for Microwave Engineering, McGraw-Hill, 1999.
[4] Pozar, Microwave engineering, John Wiley & Sons, 1998.
[5] Agilent's Advanced Design System 2006A